KERNFORSCHUNGSZENTRUM

KARLSRUHE

September 1969

KFK 1036
EUR 4309 e

Institut für Angewandte Reaktorphysik

The Measurement and Calculation of the Reactivity Worth of Samples in a Fast Heterogeneous Zero Power Reactor

W.J. Oosterkamp

GESELLSCHAFT FUR KERNFORSCHUNG M.B.H.

KARLSRUHE

KERNFORSCHUNGSZENTRUM KARLSRUHE

September 1969

KFK-1036
EUR 4309 e

Institut für Angewandte Reaktorphysik

THE MEASUREMENT AND CALCULATION OF THE REACTIVITY WORTH OF SAMPLES IN A FAST HETEROGENEOUS ZERO POWER REACTOR

W.J. Oosterkamp

Gesellschaft für Kernforschung mbH., Karlsruhe

Work performed within the association in the field of fast reactors between the European Atomic Energy Community and Gesellschaft für Kernforschung mbH., Karlsruhe

Als Dissertation genehmigt von dem Promotor Prof. Dr. M. Bogaardt, T.H. Eindhoven.

ABSTRACT

A method is developed to account for sample size and environmental effects of reactivity worth experiments - danger coefficients - in heterogeneous zero power reactors. The method bases on a perturbation expression of integral transport theory in the multigroup collision probability formulation. The method accounts for space-dependent resonance self-shielding.

A pile-oscillator element is described that only slightly perturbs the slab geometry of the reactor. The experiments can therefore be interpreted with an one-dimensional model.

The inverse kinetics method is extended to account for periodically moving fuel.

Theory and experimental equipment have been tested in a series of measurements in SNEAK- The theory and the results of the perturbation expression of diffusion theory are compared for these experiments.

KURZFASSUNG

Es wurde eine Methode entwickelt, die Probengrößen- und Umgebungseffekte bei Materialwertmessungen in heterogenen schnellen Reaktoren berücksichtigt. Die Methode basiert auf einem Störungsausdruck der integralen Transporttheorie in der Stoßwahrscheinlichkeitenformulierung. Die Methode berücksichtigt ortsabhängige Resonanz-Selbstabschirmung.

Ein Pile-Oszillator-Element wird beschrieben, welches die Plattengeometrie des Reaktors nur wenig stört. Die Experimente können deshalb mit einem eindimensionalen Modell nachgerechnet werden. Die inverse kinetische Methode wurde erweitert, um periodisch bewegten Brennstoff zu berücksichtigen. Theorie und experimentelle Methode wurden in einer Reihe von Messungen in SNEAK getestet. Die entwickelte Theorie und der Störungsausdruck der Diffusionstheorie werden für die Experimente verglichen.

1. INTRODUCTION

1.1 Preface

Fast reactors may become a major power source in the future. For the layout and safety analysis of fast power reactors it is necessary to know a number of parameters. These describe the neutron physical behaviour. The critical mass, the enrichment of the fuel, the power distribution, the worth of control rods, the breeding gain, and the temperature coefficients are the most important of these parameters.

The calculation of these quantities for fast reactors is generally more difficult than for thermal reactors, the important reaction rates occur over a larger energy range. The nuclear calculations require a detailed knowledge of the cross sections in the energy range of 1 eV to 10 MeV. Up to now there exist large uncertainties in these microscopic data, especially for the higher isotopes of the fertile and fissile materials but in certain energy ranges also for the main constituents of the reactor.

These uncertainties in the nuclear data, and also those caused by simplifying models, are still too large to calculate fast power reactors parameters with an accuracy that is sufficient for the safety analysis and economical optimalisation. Integral experiments can diminish these uncertainties.

The calculational methods and the condensed nuclear data - so called group constant sets - may be systematically tested and improved by the measurement of integral parameters.

Zero power reactors represent neutron physical models of future breeder reactors. They work at lower power and, therefore, the problems associated with heat removal and intense radiation do not exist. Their construction allows the simulation of a large number of different compositions for future power reactors. The zero power reactor SNEAK in Karlsruhe has been described in /1/.

Zero power reactors cannot exactly simulate the neutron physical behaviour of future power reactors. It is believed, however, that in the case that the calculational methods and data sets predict integral measurements in zero power reactors sufficiently well they may also predict these parameters in power reactors with the required accuracy.

Reactivity worth measurements - also called danger coefficient measurements - form one kind of integral measurements that are suited to diminish the uncertainties in the safety analysis and economical optimalisation.

These measurements are performed by measuring the variation in reactivity - multiplication factor - after insertion of a sample. In the world's first reactor, the Chicago Pile No. 1 (also a zero power reactor), these measurements were performed to measure the absorption cross sections of different materials /2/.

Since then reactivity measurements in thermal reactors have become a tool in material analysis. Homogeneity, purity, and burn up of samples are determined by this method /3,4/.

Reactivity worth measurements in fast reactors may be classified as follows:

Technical Measurements

They are used in the layout and safety analysis of fast reactors.

- Coolant loss reactivity measurements
  (These require a high accuracy because the coolant loss reactivity is an important safety parameter and also influences the stability of the reactor.)
- Determination of burn up effects
- Determination of the effectivity of absorbing materials for control rods
- Determination of small layout variations, e.g. the effect of adding steel.

Physical Measurements

These are performed to test calculational methods and nuclear data sets.

- Determination of the adjoint flux in the resonance region
  (The adjoint flux (importance) can be measured by means of neutron sources down to 2 keV. A combination of reactivity and absolute activation measurements of resonant absorbers will produce information with respect to the adjoint flux in the resonance region. Mn has been used for this purpose /5/.)
- Obtaining information on cross sections
  (This will be the emphasis of this study.)

The k_{eff} calculations of the future fast reactors should have an accuracy of 0.5%, which is the uncertainty in k_{eff} caused by the fabrication tolerances, enrichment of the fuel etc. With the present methods and cross section sets the estimated accuracy in the calculations is 2% /6/. This is mainly caused by errors in cross sections.

The cross section sets in use in Karlsruhe are based on the evaluation of differential measurements /7/. The improvement of present modifications is only minimal as far as k_{eff} is concerned. In order to predict k_{eff} for the designed prototype of the Na-cooled fast breeder that should become critical in 1974 with the desired accuracy, integral measurements should be used to improve the present cross section sets. This type of cross section adjustment has been successfully used by Pendlebury and Rowlands in England and Barré in France /8, 9, 10, 11/.

If a cross section set adjusted in this manner calculates correctly a large variety of assemblies it may safely be assumed that the error made in calculating unknown assemblies will not be too large. If errors caused by the calculational methods are off-set by cross section adjustments this too will introduce no large errors for k_{eff} calculations as long as the difference between the calculated and the measured assemblies is not too large. The more different integral measurements of sufficient accuracy are available for corrections the more reliable the adjustments are.

Reactivity measurements of samples are a means to obtain integral data quickly compared to the time required to build an assembly. If the measurements of the same materials are repeated with different spectra energy dependent integral cross sections or cross section adjustments may be obtained /12/.

Inconsistencies between calculational and experimental methods for sample reactivities or reaction rates cause false adjustments to be made. These may cause false k_{eff} predictions.

1.2 Qualitative Description of the Effects

In practivally all fast zero power reactors the composition of future fast breeder reactors is simulated by platelets of fixed composition, e.g. PuO_2/UO_2, canned Na, steel etc. This results in heterogeneity effects. The effect of heterogeneity in k_{eff} is generally not too large. What happens if a sample is inserted in such a plate type reactor depends on the material of the sample.

- An absorbing material with a high absorption cross section will absorb so many neutrons that the flux in the sample will be more or less depressed depending on the distance to the surface (self-shielding). The reaction rate and thus the reactivity effect per gramme of the sample will be smaller for a thicker sample than for a very thin one.
- If the sample is a fissionable material, fission neutrons born in the sample have a probability to cause another fission in the sample (self-multiplication). The fission rate and the reactivity effect per gramme will therefore be larger in a thicker sample than in a small sample.
- The reaction rate in a resonance material will mainly come from the resonances - this is true if the flux in the resonance region is still substantial as is the case in ceramic fueled fast reactors. The reaction rate will therefore be less if the flux is depleted in the resonances. This is the case if the same material is in the neighbourhood of the sample. Thus the reactivity effect per gramme of a sample will not only depend on the thickness of a sample, but also whether or not the same material is contained in the neighbouring platelets.
- The flux of neutrons that have collided with a scattering material generally shows no strong energy dependency since the resonance width is small compared with the average lethargy gain per collision. The probability for absorption of these neutrons will therefore be higher than for non-collided neutrons. The flux of the latter will show dips in the resonances, in the case that a resonance absorber is in the neighbourhood of the sample.

A good theory must be able to describe these effects.

1.3 Limitations of the Methods Presently in Use

Perturbation theory as it is used is inadequate to describe these effects /13/. For B10 with the large absorption cross section it is clear that self-shielding is of importance in large samples. For resonance materials self-shielding is of importance in the resonances. The self-shielding factors of the perturbing cross sections should lie between those of the core and of the pure sample material, if the concept of Abagjan et al. is used /14/. The exact value is difficult to estimate since it depends on the thickness of the sample and the composition of the environment.

In /15/ E.A. Fischer describes a computer code that calculates by means of collision probabilities correct self-shielding factors in the case that the core can be treated as homogeneous. This code takes also into account self-shielding, self-multiplication, and multiple scattering in the sample. Since Fischer treates the reactor as homogeneous no account is taken of the differences in depletion of the impinging flux by the resonances when the same material as the sample is in close vicinity.

In Argonne a groupwise correction for self-shielding by means of collision probabilities is made in the evaluation of reactivity measurements of samples /16/. Since the groups are wide compared to the resonance width, for resonance materials no improvement is made by this method. To obtain a good correction the group width should be small compared to the resonance width, and then the flux fine structure of the impinging flux should be known.

The elaborate method of P.E. McGrath and W.K. Foell will, for the same reason give no improvement /17/. They too use broad groups.

The computer codes Rabble and Rabid developed by Kier and others in Argonne can correctly describe this phenomena /18/. The codes are based on integral transport theory for a number of zones and the group width is small compared to the average lethargy gain per collision, so space dependent self-shielding is accounted for. The codes use, however, so much computer time that they are not even used for routine heterogeneity calculations /19/. It is therefore unlikely that they can be used for routine reactivity calculations for samples. This type of code is not yet available in Karlsruhe.

1.4 Aim of and Means for this Study

The discrepancies between theory and experiments for reactivity worth measurements have been large. Generally it is now agreed not to use these measurements for the improvement of cross section sets /20/.

For a number of cross sections, e.g. those of the higher isotopes of plutonium and of the structural materials these measurements are the only integral test possible with zero power reactors.

The aim of this study, the results of which are presented here, was to improve the experimental methods and the theory in such a way that the remaining discrepancies between theory and experiment are caused by errors in the cross section sets only.

We discussed already the important effects on the reactivity worth of a sample. A perturbation expression of integral transport theory as described by E.A. Fischer /21/ seemed apt to calculate these heterogeneity effects correctly. But the averaging process to obtain reaction rates for space dependent resonance self-shielding would be extremely time consuming. A special data compilation would be necessary. Therefore this method would be of no value to test data sets for standard reactor calculations. The ZERA code of D. Wintzer /22/ corrects the reaction rates for the homogenized medium, as calculated by standard methods, for the space dependent resonance self-shielding. This code is not suited for sample calculations because a homogeneous case cannot easily be defined for these calculations. A number of modifications had to be made to remove this limitation and to adapt the code to the perturbation expression.

The computer code REAC (Reactivity Calculation) that incorporates the modified ZERA code solves the perturbation expression.

Thus reactivity worth measurements of samples can be calculated by integral transport theory including the effect of space dependent resonance self-shielding.

In this study a different approach has been developed for the calculation of reaction rates. It does not have the inconsistencies still present in the modified ZERA code and it is better suited for the perturbation expression of integral transport theory.

The large discrepancies between theory and experiments may partly be explained by the fact that large samples were used and evaluated with perturbation theory for diffusion calculations. Perturbation theory is valid for very small samples only. Small samples should be preferred even if better calculationsal methods are used, because the interpretation is easier.

In order to enable the calculation of environmental effects, a simple geometry should be chosen. The normal loading pattern of SNEAK is in slab geometry. The mechanism to bring the sample in and out of the reactor - the pile oscillator - has been constructed anew so that this slab geometry is practically only perturbed by the sample itself.

Thus the pile oscillator is loaded with the normal pattern of the reactor. It is moved periodically in order to eliminate linear drift of the reactor.

Periodically moving fuel gives a pseudo reactivity effect if the reactivity is calculated from the variation of the flux by the inverse kinetics method of Carpenter /23/. A theory has been developed to correct for this effect. The computer programme KINEMAT is based on this theory.

The interpretation of the experimental results has not yet been formalized. However, a scheme is proposed to obtain improved cross section sets from the experimental reactivity worth experiments.

2. THEORY

In this chapter a method for the calculation of collision and reaction probabilities is developed taking into account the effect of space-dependent resonance self-shielding. A perturbation expression for the integral transport theory is derived in the collision probability formulation. The perturbation expression will be so formulated that it can be compared to the perturbation expression of diffusion theory. The latter is the standard method for sample reactivity calculations. The differences of the two expressions will be discussed.

A formulation of transport theory has been chosen, because diffusion theory is in error for strongly absorbing media.

2.1 Reaction Probabilities

The reaction rate $R_x(E,r)$ in a point r of a reaction of the type x - e.g. fission capture, scattering - induced by neutrons with the energy E can be expressed by the source distribution in the whole reactor /12/. We can write the reaction rate in the following multigroup formulation if we assume that the sources are isotropic and only a slowly varying function of energy - narrow resonance approximation /25/.

$$R_{xi}(r) = \int_V dV'\ S_i(r') < P_x(E,r' \to r) >_i \qquad (2.1)$$

$R_{xi}(r)$ is the reaction rate of a reaction of the type x at the point r of neutrons with the energy of the group i

V is the volume of the reactor

$S_i(r')$ is the source density of neutrons with the energy of the group i at the point r'

$< >_i$ denotes the averaging over the energies of the group i

$R_{i \to j}(r)$ is the moderation rate. It is the rate at which neutrons of the energies of the group i are scattered down to the energies of the group j

$P_x(E,r' \to r) = \Sigma_x(E,r) \dfrac{e^{-1(E)}}{4\pi |r'-r|^2}$ is the reaction probability

It is the probability that a neutron of the energy E starting isotropically at r' will make a reaction of the type x at r

Σ_x is the macroscopic cross section for the reaction x

$1(E) = \left| \int_{r'}^{r} dr'' \, \Sigma_t (E,r'') \right|$ is the number of mean free paths

Σ_t is the total macroscopic cross section

In a homogeneous medium

$$1(E) = \Sigma_t(E)|r'-r| \tag{2.2}$$

No averaging of the reaction probabilities is needed if the variations of the macroscopic cross sections with energy in a group are small enough. In the resonance region this requires a small group width compared to the resonance width. It would mean that over the energy range of ceramic fueled reactors more than 10 000 groups are needed. This large number is at the moment not feasible.

The reaction probability is a function of geometry and macroscopic cross sections and only implicitly of energy. It is, however, a function of the toal macrosopic cross sections of all the media between r' and r.

The macroscopic cross section is given by

$$\Sigma_x^m (E) = \sum_{y=1}^{Y} N^{ym} \cdot \sigma_x^y(E) \tag{2.3}$$

m denotes the medium

y denotes the isotope

Y is the number of isotopes

N^{ym} is the concentration of the isotope y in the medium m

σ_x^y is the macroscopic cross section of the isotope y for the reaction x.

Each medium may have a different composition and therefore a different total macroscopic cross section as function of energy. The situation is simplified if we assume no resonance overlap. The cross sections of the other isotopes will be a constant function of energy in those energy ranges where one isotope has a resonance.

This assumption is certainly not correct. The resonance self-shielding is, however, as Bondarenko noted in /14/ a comparatively weak function of the sum of total cross section of the other elements, so that the error made in using the potential cross section of the other isotopes as background cross sections will be small.

Codd and Collins discuss in /26/ the effect of overlap of U238 and Pu239 resonances and found that for Pu239 capture and fission the interaction with U238 resonances might be significant. This effect can be accounted for by an extension of the method described below, but this extension will not be given here.

We define now the equivalent background cross section σ_o^{ym} for a certain isotope y in a medium m

$$\sigma_o^{ym} = \frac{1}{N^{ym}} \sum_{\substack{z=1 \\ z \neq y}}^{Y} N^{zm} \cdot \sigma_t^z \,. \qquad (2.4)$$

The equivalent background cross section is independent of energy within a group in those ranges where the isotope y has a resonance. We approximate the total cross section of this isotope by a histogram. We add the width of steps of the same height together and divide by the width of the group. Thus we obtain the relative width α_k^y for steps of the height σ_{tk}^y of the total cross section of the isotope y. We average the cross section for the reaction x over the steps of the same height of the total cross section. Resonance isotopes have generally a large number of resonances in each group. This procedure greatly reduces, therefore, the number of points to be calculated to obtain correct values for the reaction probabilities. We may do this because steps of the same height and the same width of different energies in a group give the same contribution to the reaction probabilities. This is the case for our assumptions of constant sources as function of energy in a group - narrow resonance approximation - and no overlap of resonances of different isotopes.

The contribution of the resonances of the isotope y to the reaction probability can now be given as the sum of the contributions of the different steps.

The contribution of the non-resonant - background - cross section to the reaction probability must be split into two terms.

The first is the contribution of those energy ranges where the other isotopes in the mixture do not have resonances.

The attenuation will be larger at energies where another isotope has a resonance. It is the same as that for neutrons that react with the resonance of that other isotope.

We defined the reaction probability as the probability that a neutron starting at r' with the energy of the group i makes a reaction of the type x at r.

Thus the reaction probabilities can be given by

$$P_{xi}(r' \to r) = \sum_{y=1}^{Y} N^{y} \sum_{k=2}^{K} \alpha_i^{yk} \, \sigma_{xi}^{yk} \, \frac{e^{-1_i^{yk}}}{4\pi |r'-r|^2} +$$

$$+ \sum_{y=1}^{Y} N^{y} \left(1 - \sum_{z=1}^{Y} \sum_{k=1}^{K} \alpha_i^{zk}\right) \sigma_{xi}^{y1} \, \frac{e^{-1_i^{y1}}}{4\pi |r'-r|^2} + \qquad (2.6)$$

$$+ \sum_{y=1}^{Y} N^{y} \sum_{\substack{z=1 \\ z \neq y}}^{Y} \sum_{k=1}^{K} \alpha_i^{zk} \, \sigma_{xi}^{y1} \, \frac{e^{-1_i^{zk}}}{4\pi |r'-r|^2}$$

where

Y	the number of isotopes
K	the number of the different steps
α^{yk}	the relative width of the step k of the isotope y
σ_x^{yk}	the average cross section for the reaction x of the step k of the isotope y in barns
$\lvert r'-r \rvert$	the distance between the source and the point considered, in cm
σ_x^{y1}	the background cross section of the isotope y for the reaction x in barns
1^{yk}	the optical path between r' and r

$$1_i^{yk} = \left| \int_{r'}^{r} dr \cdot N^{ym} (\sigma_{ti}^{yk} + \sigma_{oi}^{ym}) \right|$$

N^{ym}	the concentration of y in the medium m in 10^{24} atoms/cm^3
σ_{ti}^{yk}	the height of the total cross section of the step k in barns
σ_o^{ym}	the equivalent background cross section in the medium m in barns

We introduce the reaction probability that a neutron from one zone n makes a reaction of type x in another zone m, assuming that the compositions of the media and the sources are zonewise constant.

Then

$$P_{xi}^{nm} = \int_{V_m} dV \int_{V_n} dV' \; P_{xi}(r' \to r)$$

$$= \sum_{y=1}^{Y} \sum_{k=2}^{K} \frac{\alpha_i^{yk} \, \sigma_{xi}^{yk}}{\sigma_{ti}^{yk} + \sigma_{oi}^{ym}} \cdot P^{nm} \, (\sigma_{xi}^{yk} + \sigma_{oi}^{y}) +$$

$$+ \sum_{y=1}^{Y} \left(1 - \sum_{z=1}^{Y} \sum_{k=1}^{K} \alpha_i^{zk}\right) \frac{\sigma_{xi}^{yl}}{\sigma_{ti}^{yl} + \sigma_{oi}^{ym}} \, P^{nm} \, (\sigma_{xi}^{yl} + \sigma_{oi}^{y}) \qquad (2.6a)$$

$$+ \sum_{y=1}^{Y} \sum_{\substack{z=1 \\ z \neq y}}^{Y} \sum_{k=1}^{K} \alpha_i^{zk} \, \frac{\sigma_{xi}^{yl}}{\sigma_{ti}^{zk} + \sigma_{oi}^{zm}} \, P^{nm} \, (\sigma_{xi}^{zk} + \sigma_{oi}^{y})$$

P^{nm} are the collision probabilities: the probability that a neutron starting in the zone n will make its first collision in the zone m. They are a function of the total macroscopic cross sections of all the zones between m and n; m and n included

Algorithmes to calculate collision probabilities have been published for two dimensions in /27/, for cylindrical geometry in /28, 29/, and for slab geometry in /30/.

A discussion of Wintzer's method to calculate reaction probabilities is given in the Appendix 2.

The relative widths and the average cross sections can be derived from differential data. This results in a special data set. The data sets as they are in use now, however, must be usable for sample reactivity calculations. Only in that case can reactivitiy measurementsbe used for the testing of these cross section sets.

The data sets in current use in Karlsruhe use, with a few exceptions, the scheme as proposed by Bondarenko in /14/ for the self-shielding. In this scheme effective resonance self-shielded cross sections are tabulated as a function of the effective background cross section.

It is possible to derive the relative width and the average cross sections from the data in the Bondarenko scheme.

We consider an infinite homogeneous reactor consisting of a single resonance isotope y and a diluent with a constant unit source.

The reaction rate of the type x in the isotope y in our scheme is given by

$$R^y_{xi} = \int_V dV \sum_{k=1}^{K} \alpha_i^{yk} \, \sigma_{xi}^{yk} \, \frac{e^{-(\sigma_{ti}^{yk}+\sigma_{oi}^{y})|r'-r|}}{4\pi|r'-r|^2} \qquad (2.7)$$

we get then

$$R^y_{xi} = \sum_{k=1}^{K} \alpha_i^{yk} \, \frac{\sigma_{xi}^{yk}}{\sigma_{ti}^{yk}+\sigma_{oi}^{y}} \; . \qquad (2.8)$$

The reaction rate of the type x in the isotope y in the Bondarenko scheme is given by

$$R^y_{xi} = \frac{\sigma^y_x \, (\sigma_o)}{\sigma^y_t \, (\sigma_o)+\sigma_o} \qquad (2.9)$$

where

$\sigma^y_x(\sigma_o)$ the effective cross section for the reaction x with the effective background cross section σ_o.

We choose the cross section σ^y_{tk} in the range between the potential cross section and the maximum resonance cross section. We require that for a given number of effective background cross sections the reaction rate as calculated by our scheme and calculated by the Bondarenko scheme are the same. We choose the number of these points to be the same as the numberof the steps k.

The relative widths α_i^{yk} are then determined by the equations

$$R^y_{ti} \, (\sigma_o) = \frac{\sigma^y_{ti}(\sigma_o)}{\sigma^y_{ti}(\sigma_o)+\sigma_o} = \sum_{k=1}^{K} \alpha_i^{yk} \, \frac{\sigma_{ti}^{yk}}{\sigma_{ti}^{yk}+\sigma_{oi}} \; . \qquad (2.10)^{+)}$$

The average cross sections by

$$R^y_{xi} \, (\sigma_o) = \frac{\sigma^y_{xi}(\sigma_o)}{\sigma^y_{ti}(\sigma_o)+\sigma_o} = \sum_{k=1}^{K} \alpha_i^{yk} \, \frac{\sigma_{xi}^{yk}}{\sigma_{ti}^{yk}+\sigma_o} \; . \qquad (2.11)$$

The accuracy for other values of the effective background cross sections is thus determined by the number of steps k. The computer time necessary to

---

+) The quantity $\alpha_i^{yk} \cdot \sigma^y_{tk}$ is then a stepwise approximation of the inverse Stieltjes transform of the collision density /31/

$$R(\sigma_o) = \int_o^\infty \frac{\alpha_i^y(\sigma_t)\sigma_t}{\sigma_t+\sigma_o} \, d\sigma_t$$

calculate the reaction probabilities is also largely dependent on the number of steps. No gain in accuracy is, however, obtained by increasing the number of steps over say 10. The effective cross sections are given for 7 values of the effective background cross sections. For other values an interpolation formula is given. This formula is not too accurate.

The theory developed here allows the correction of the reaction rates for the space-dependent self-shielding. Thus correction factors for heterogeneity can be given as required by the extension of the Bondarenko scheme by Bitelli /32/. It is however not in the scope of this study to discuss the accuracy and limitations of this extended scheme.

2.2 The Perturbation Expression

The perturbation expression of integral transport theory is according to E.A. Fischer in /24/ given by Eq. 2.16. In the next paragraph its derivation is outlined.

The group sources in a reactor where the spontaneous source can be neglected are given by the fraction χ_i of the fission neutrons that are born in the group times the average number of fission neutrons per fission, ν, times the fission rate plus the moderation rate in that group.

Thus we get

$$S_i(r) = \chi_i \sum_{j=1}^{G} \nu R_{fj} + \sum_{j=1}^{i-1} R_{j\to i} \qquad (2.12)$$

G is the number of groups

For a critical reactor, we can express the reaction rates through the sources with Eq. 2.1 and obtain theintegral transport equation in the collision probability formulation

$$S_i^m = \int_{V_n} S_i(r)dV = \sum_{m=1}^{M} \{\chi_i \sum_{j=1}^{G} \nu P_{fj}^{nm} S_j^n + \sum_{j=1}^{i-1} P_{j\to i}^{nm} S_j^n\} \qquad (2.13)$$

M is the number of zones

The adjoint equation is

$$S^{+n} = \sum_{m=1}^{M} \{ \sum_{j=1}^{G} \chi_j \, S_j^{+m} \, \nu \, P_{fi}^{nm} + \sum_{j=i}^{G} S_j^{+m} \, P_{i\to j}^{nm} \} \qquad (2.14)$$

The adjoint source $S_i^+(r)$ can be interpreted as the probability that a neutron starting in n with the energy of the group i will eventually produce a fission neutron.

We assume that there are small perturbations δP_{xi} in the reaction probabilities

$$P_{xi}^{nm} = P_{xi}^{onm} + \delta P_{xi}^{nm} \qquad (2.15)$$

and that the effect of these $\delta P_{xi}(r\to r')$ is compensated by a change $\delta\nu$ in ν. Then we obtain by standard manipulations the following expression for the reactivity effect of the perturbation

$$-\frac{\delta\nu}{\nu} = \frac{1}{F} \sum_{n=1}^{M} \sum_{m=1}^{M} \sum_{i=1}^{G} \{ \sum_{j=1}^{G} \chi_i S_i^{o+m} \nu \delta P_{fj}^{nm} \, S_j^n \sum_{j=1}^{i=1} S_i^{o+m} \, \delta P_{j\,i}^{nm} \, S_j^n \} \qquad (2.16)$$

where

$F = \sum_{n=1}^{M} \sum_{m=1}^{M} \sum_{i} \sum_{j} \chi_i \, S^{o+m} \, \nu \, P_{fj}^{nm} \, S_j^n$ is the normalisation integral

S^m are the sources in the perturbed reactor

S^{o+n} are the adjoint sources in the unperturbed reactor

This expression is rigorous except for the approximation of isotropic scattering, the narrow resonance approximation, and the condition of no overlap of resonances of different isotopes.

In the appendix and in /29/ a more detailed derivation is given.

In order to compare this equation with the standard perturbation equation of diffusion theory we discuss the following problem: The unperturbed case is the reactor with the sample in the in position. The perturbed case is the reactor with the sample in the out position. Leackage is accounted for by introducing a black absorber as outmost zone. We assume that the sources are only slightly perturbed except those of the sample position. This zone is the zone no. 1.

The neutrons that would have collided in the sample now collide in one of the core zones, since each source neutron must collide somewhere.

$$\delta P_i^{n1} \, S_i^n + \sum_{j=i}^{G} \delta P_{i\to j}^{n1} \, S_i^n = -\sum_{m=2}^{M} \{ \delta P_{ai}^{nm} \, S_i^n + \sum_{j=i}^{G} \delta P_{i\,j}^{nm} \, S_i^n \} \qquad (2.17)$$

P_a is the reaction probability for absorption, i.e. capture plus fission

We may now define the probability to produce eventually an extra fission neutron for these neutrons S_i^{+c} as the average probability to produce a fission neutron when they do not collide with the sample

$$S_i^{+c} = Df \frac{\sum_{n=2}^{M} \sum_{m=2}^{M} \{\sum_j \chi_j S_j^{+m} \delta P_{fi}^{nm} S_i^n + \sum_{j=i}^{G} S_j^{+m} \delta P_{i\to j}^{nm} S_i^n\}}{\sum_{n=2}^{N} \sum_{m=2}^{N} \{\delta P_{ai}^{nm} S_i^n + \sum_{j=i}^{G} \delta P_{i\to j}^{nm} S_i^n\}} \quad . \qquad (2.18)$$

The perturbation equation 2.16 may be split into two parts. The first is the reactivity loss of the neutrons that would have collided with the sample. The second term is the reactivity gained by these neutrons in the rest of the core. This second term may be expressed using the definition of the core adjoint in noting that the denominator of (2.18) may be simplified by Eq. 2.17 and in making use of the fact that in the perturbed case the source of zone one is zero(void)

$$-\frac{\delta\nu}{\nu} = \frac{1}{F} \sum_{i=1}^{G} \{ \sum_{j=1}^{G} \chi_j S_j^{+1} \sum_{n=2}^{M} \delta P_{fi}^{n1} S_i^n - S_i^{+c} \sum_{n=2}^{M} \delta P_{ai}^{n1} S_1^n +$$

$$+ (S_i^{+1} - S_i^{+c}) \sum_{n=2}^{M} \delta P_{i\to i}^{n1} S_i^1 + \sum_{j=i+1}^{G} (S_j^{+1} - S_i^{+c}) \sum_{n=2}^{M} \delta P_{i\to j}^{n1} S_j^1 \}. \qquad (2.19)$$

We will now discuss the different terms. We note first that we called the reactor with the sample"in"the unperturbed case. We now revise this by changing the sign of the reactivity change

$$\frac{\delta\nu}{\nu} = \frac{1}{F} \sum_i \{A_i + B_i + C_i + D_i\} \qquad (2.20)$$

where

$A_i = \sum_j \chi_j S_j^{+1} \sum_{n=2}^{N} \delta P_{fi}^{n1} S_1^n$ is the reactivity gain caused by the fissions in the sample

The effect of self-multiplication is taken account of by the probability to produce a fission neutron S_j^{+1}. This probability is calculated anew for each sample.

$$B_i = -S_i^{+c} \sum_{n=2}^{M} \delta P_{ai}^{n1} S_i^n$$

is the reactivity loss caused by the absorptions in the sample.

$$C_i = (S_i^{+1} - S_i^{+c}) \sum_{n=2}^{M} \delta\, P_{i\to i}^{n1}\, S_i^n$$

is the difference in reactivity caused by neutrons that are scattered in the sample without being transferred to the next group.

The difference in the probability to produce a fission neutron is due to the fact that the neutrons that collide in the sample have a higher probability to be absorbed in the resonances of the sample and the core than non-collided neutrons. The flux of the latter shows dips at the energies of the resonances. After a collision these dips are filled up. The probability of being absorbed is especially large for those neutrons that have the energy of a resonance.

For U238 this effect is of importance. U238 is a resonance absorber and one would expect a strong sample size effect. The elastic scattering in a U238 sample makes the effect smaller. The flux depression in the sample is partly filled up with elastically moderated neutrons. These neutrons, therefore, have a high probability of being captured in the sample. This probability increases with increasing thickness.

$$D_i = \sum_{j=i+1}^{G} (S_j^{+1} - S_i^{+c}) \sum_{n=2}^{M} \delta\, P_{i\to j}^{n1}\, S_1^n$$

is the difference in reactivity caused by the moderation of the neutrons in the sample.

$$R_{xi}^{1c} = \sum_{n=2}^{N} \delta\, P_{xi}^{n1}\, S_1^n$$

is the total reaction rate in the sample of neutrons that come directly from the core.

In the standard perturbation theory this reaction rate is given by the cross section of the sample times the flux integrated over the sample. We define now an effective cross section

$$R_{xi}^{1c} = \sum_{n=2}^{M} \delta\, P_{xi}^{n1}\, S_i^n = \delta\, \Sigma_{xi}^{eff}\, \Phi_i\, \Delta V$$

where

Φ_i the unperturbed flux of the diffusion theory

ΔV the volume of the sample

Eq. 2.20 can than be written

$$\frac{\delta\nu}{\nu} = \frac{\Delta V}{F} \sum_{i=1}^{G} \{ \sum_{j=1}^{G} \chi_j \, S_j^{+1} \, \delta \, \Sigma_{fi}^{eff} \, \Phi_i - S_i^{+c} \, \delta \, \Sigma_{ai}^{eff} \, \Phi_i +$$

$$+ (S_i^{+1} - S_i^{+c}) \, \delta \, \Sigma_{i\,i}^{eff} \, \Phi_i + \sum_{j=i+1}^{G} (S_j^{+1} - S_i^{+c}) \, \delta \, \Sigma_{i\,j}^{eff} \, \Phi_i \} \qquad (2.21)$$

This equation is similar to the standard multigroup perturbation equation

$$\frac{\delta\nu}{\nu} = \frac{\Delta V}{F} \sum_{i=1}^{G} \{ \sum_{j=1}^{G} \chi_j \, \Phi_j^{+} \, \delta \, \Sigma_{fi} \, \Phi_i - \Phi_i^{+} \, \delta \, \Sigma_{ai} \, \Phi_i + \sum_{j=i+1}^{G} (\Phi_j^{+} - \Phi_i^{+}) \, \delta \, \Sigma_{i \to j} \, \Phi_i \} \qquad (2.22)$$

The difference to the standard perturbation theory can be sumarized as follows:

- The effective cross sections account for space-dependent self-shielding in the sample.
- The adjoint of the core S^{+c} takes account of the resonance structure of the probability to cause a fission. The adjoint of the core will be different for different samples depending on whether the neutrons that collide in the sample come mainly from the resonances or not. Thus the core adjoint for U238 will be lower than for B10 because the neutrons that collide with U238 stem mainly from the resonance energies of U238 and would have partly been captured anyway whereas for B10 it is a smooth average over energy.
- The difference in adjoint for neutrons in the core and in the sample.

The theory developed here gives us an understanding of the effects and enables us, to take space-dependent resonance self-shielding in the calculation of the reactivity effects of small samples into account.

The Eq. 2.13 and 2.14 plus the Eq. 2.19 have been programmed in FORTRAN II for the IBM 7074. For the calculation of reaction probabilities a modification of the ZERA code /30/ is used. The application of this theory to experiments will be discussed later on in this paper.

3. EXPERIMENTAL METHODS AND EQUIPMENT

We will discuss now the equipment and the methods used to make high precision reactivity experiments that can be easily interpreted.

3.1 The Pile-Oscillator

In practically all fast zero power reactors the sample reactivity measurements are performed in such a way that the normal lattice is strongly perturbed. About 3 mm steel was introduced in the direct environment of the samples by the oscillator element and its guiding tube in SNEAK /1/. This element moves the sample into and out of the reactor. The steel influences the measured reactivity effect of U238 by about 10% /34/. The platelets by which the reactor compositions are simulated had a different orientation in the vicinity of the sample than elsewhere where they laid horizontally.

The calculations should be made with a three-dimensional model in order to represent closely the complicated geometry of the experiment.

As to simplify the geometry we have developed a special vertical pile oscillator element (Fig. 1) that uses an existing pneumatic drive. It consists of a square tube 47·47 mm^2 with 1 mm wall thickness and moves in a guide tube of the same thickness. In the upper half o.5 mm thick SS bridges have been welded in the oscillator tube at distances of 50 mm. Between the bridges and in the lower half platelets can be introduced. In the upper half they can easily be exhanged because the SS bridges subdivide the oscillator tube in small compartments.

The main feature of the set up is that the platelts lie so that in general the slab geometry of the core is not perturbed. The bridges and boxes that contain the platelets have been designed in such a way that they come in lieu of the SS platelets that form part of the lattices. The only larger perturbations of the core are formed by the guiding tube and the sample. It is, however, a good approximation for thin samples to describe the geometry with an one-dimensional model.

The oscillating element is connected to the piston of a driving mechanism actuated by compressed air. The stroke of the oscillator is 80 cm so that the sample can be moved from the centre of the core to a position outside the blanket. The transient time between both positions is three seconds such that the reactivity approximately is changed in a square wave manner with a period of 120 sec.

3.1 Reactivity Determination

An existing linear flux measuring channel is used to measure the variation in the flux. As detector a large BF_3 chamber is positioned at the outer edge of the reactor blanket of depleted uranium. The ion chamber is surrounded with polyethylene plates in order to raise its sensitivity to a high enough value that the detection noise in the chamber is smaller than the fluctuations caused by reactor noise. In this way the theoretical precision limit of measured reactivity that can be reached at a certain reactor power within a certain length of time is closely approached. The amplifier uses voltage dependent capacitors in its input. Zero drift is negligible, and the overall linearity was measured to be within 0.03%.

In order to allow digital treatment of the flux data the output voltages of the amplifiers are digitized by voltage to frequency converters. The output pulses of these ADC's are counted during a certain time interval. The DDP 124 computor allows on-line calculation and plotting of reactivity with a digital plotter even with the extended version of inverse kinetics calculation of reactivity that is described briefly below.

The utilisation of the inverse kientics method offers for oscillating measurements over Fourier analysis the advantage that each data point is treated separately, so that false counts (e.g.zero) can easily be detected and, sencondly, that a drift correction can be made separately for each period. Transients, e.g. when a sample traverses the reactor core, are treated correctly by the program and do not influence the computed reactivities of the "in" and the "out" position.

Several extensions have been made to the program that solves the inverse kinetics equations.

It is necessary to fill the pile oscillator with core material in the vicinity of the sample if one does not want to perturb the slab geometry of the reactor. In order to avoid large reactivity transients during sample traverses the oscillator should be filled completely with the same material. Not only fissionable material, but also the delayed neutron precursors that have been built up in it are moved with the drawer to locations with different importance. This effect is not treated by the point kinetics equations; they have therefore been extended in such a way that this effect is taken into account. The point kinetics equations can be used for the

description of a multizone reactor if one gives the variables effective values which are composed of the variables of separate reactor zones by weighting them with the adjoint fluxes in these zones (see appendix). Conditionsfor the applicability of extended point kinetics is that the fission rate distribution remains constant, which is the case when a homogeneous drawer moves. In a zone where fuel moves the change of the precursor concentration is given by production minus decay plus net transport

$$\frac{dC_i}{dt} = \beta_i \, k(t) \, \frac{n(t)}{l} - (\nabla C_i(t,\vec{r}), \vec{v}(t,\vec{r})) - \lambda_i C_i(,\vec{r}),$$

in which $\vec{v}$ = the velocity of the fuel, $\vec{r}$ = position.

This is taken into account for the channel through which the pile oscillator moves in the KINEMAT code. The channel is divided in a number of zones, and the precursor concentrations are calculated for each counting interval. With this computation the initial drift of the reactivity steps that is shown in Fig.2 disappears.

It is now meaningful to calculate the standard deviation of each step in order to determine the influence of reactor statistics. Large differences in standard deviations of consecutive steps are an indication of gross deviations in count rates, e.g. caused by electronic failures or punching faults. The occurance of false count rates is serious, since they influence the reactivity computation at later times. In order to eliminate such faults an optional routine has been added to the program that eliminates those count rates that deviate more than two times the standard deviation from the five previous values or do not lie either below the maximum or above the minimum of 5 following countrates. A countrate that is considered as false by these criteria is replaced by the average of the previous and the following values. This routine can only be applied when no reactivity peaks of short duration occur. Optionally the computer program can plot all reactivity values with a digital plotter.

All measured sample worths are corrected for linear reactor drift by averaging the reference positions before and after the "sample-in" position. The actual dirft of the "sample-out" reference positions is also tested for linearity, and nonlinear dirft contributions are taken into account as additional terms in the error calculation. This KINEMAT code is now in routine use and works to complete satisfaction /35/.

3.3 The Effect of Uncertainties in the Delayed Neutron Parameters on the Reactivity as Calculated by the Inverse Kinetics Method

The reactivity as calculated with the inverse kinetics method is given in dollar. One dollar is the effective fraction of delayed neutrons. Errors are introduced by the uncertainties in the fractions of the different groups of delayed neutrons and in the half lives of the precursor nuclei. These errors have been studied by first solving the in-hour equation /24/ for a certain reactivity step. This gave the flux a function of time. Then the reactivity was calculated by the inverse kinetics method with somewhat changed kinetic parameters. The differences between the input reactivity and the calculated reactivity was small.

3.4 Experimental Determination of the Ratio of the Effective Delayed Neutron Fraction and the Normalisation Integral

The effective fraction of delayed neutrons β and the normalisation integral F of the Eq. 2.16 should be known in order to compare measurements and calculations. They are both determined by the properties of the whole reactor. Specially in Pu fueled reactors β is markedly influenced by the fissions in U238. Fissions in the blanket should be taken into account also. In a radial one-dimensional calculation in cylinder geometry only the radial blanket is taken into account; in spherical geometry a cylindrical reactor is not well represented either. One-dimensional β and F calculations as they are presently made are therefore too inaccurate.

A possibility to overcome this is to normalize the calculated reactivity worths with the reactivity worth of a well known isotop, e.g. U235. Then, however, errors in the cross section of this isotop can not be detected and they will erroneously be attributed to other isotopes.

A different possibility is a combination of fission rate measurements and an effective source determination of a calibrated source with a spectrum similar to that of fission neutrons. The exact formula for this method is derived in the appendix.

3.5 Interpretation of the Results

Theory and experimental methods have been modified in this study so that the model for the calculations closely represents the experimental situation. We assume therefore that discrepancies between theory and experiments may be attributed to cross section errors only.

It is, however, not obvious how much the cross sections should be altered to improve the agreement between experiments and calculations. Changes in cross sections of core materials will necessarily alter the spectrum and the adjoint spectrum and thus all reactivity calculations should be repeated.

It is much better to make the calculations with experimental spectra and adjoint spectra. The spectrum can be measured with proton recoil and sandwich measurements. The adjoint spectrum can be measured with neutron sources and with a combination of reactivity measurements and absolute activation measurements. The last method must still be developed to be practical.

With proton recoil and the neutron source measurements no local fine structure of spectra and adjoint spectra can be measured. The accuracy of the sandwich foil technique and the activation technique is much smaller than that of the material worth measurements. So that this method is not practical either.

A somewhat different approach can be followed if a simplified model is used. This may be a homogeneous zero-dimensional multigroup calculation. From a correct calculation with a guessed cross section set in which space-dependent self-shielding is accounted for correction factors may be obtained for the reaction rates in the model. In the same way correction factors may be obtained for the sample reactivity calculations.

The cross sections may then be varied until the calculated results of the model and the experimental results agree within the error limits. The sample reactivity calculations can then be made with the extended method and the new cross section set. If necessary this procedure may be repeated.

It is expected, however, that the correction factors in a multigroup representation depend only in second order on the cross sections used.

4. EXPERIMENTS

The first series of experiments that were performed as described in this study were done in the assembly SNEAK-5C. This assembly is extensively described in /36/. It was built to determine the capture to fission rate of Pu239. The median fission energy was 500 eV. The main constituents were graphite, natural uranium and plutonium.

The assembly was very heterogeneous. The optical thickness of the graphite was 1 1/2 mean free pathes. The heterogeneity correction in k_∞ was 7% in k.

It was,however, an ideal assembly to test the methods developed because of the soft spectrum and the large heterogeneity.

The measurements were made at two positions in the lattice (see fig. 3) to study environmental effects. Special attention was paid to sample size effects.

The standard deviation of the measurements reached the theoretical lower limit as calculated by Cohn /37/, where only statistical fluctuations of the neutron population in the reactor are considered ("reactor noise"). The reproducibility of the measurements was inside the range given by the standard deviation of each measurement. The standard deviation of the experiments is 10 µ$. This is equivalent with the worth of 25 mg Pu239 or 400 mg U238.

4.1 Interpretation of the Experimental Results

The results of the measurements - in so far as they are important for our study - are given in the Figures 4 and 5 and in the Table 1. The values are given in µ$/g and have been corrected for the other isotopes present in the sample by measured values for these isotopes.

The neutron spectrum at the position 1 has no resonance structure. The neutrons, that collide with the sample made their last collision in graphite and none have been filtered out by resonance isotopes. The sample size effect for U238 is very pronounced. The effect is caused by the resonance self-shielding in the sample itself (Fig. 6).

The neutron spectrum at the position 2 has a pronounced resonance structure. Neutrons with energies of U238 and partly of Pu239 have been filtered out by these isotopes that are adjacent to this position. The neutrons from non-resonance energies will therefore give the main contribution to the reactivity effect of U238. Part of the effect comes from the elastic scattering of neutrons by the sample from non resonant energies to energies of U238 resonances by which they are captured. The sample size effect is thus not large.

The sample size effect of Pu239 in the graphite is much less than that of U238. The samples consist of PuO_2 and Fe in the form of pellets. The diluents oxygen and iron give an equivalent background cross section of approximately 10 barns. The self-shielding effects are for this background cross section much less pronounced than for the pure material. The range covered by the measurements is also smaller than that covered by the U238 measurements.

The spectrum at the position 2 has only a weak resonance structure caused by Pu239 resonances - though U238 resonances introduce a pronounced resonance structure - we have plutonium only on one side of the sample, so that only these neutrons contribute to the resonance structure of the spectrum. The plutonium is present in a mixture of UO_2 and PuO_2 and the equivalent background cross section is 100 barns, so that the self-shielding is not too large.

The major difference of the positions 1 and 2 with regard to the reactivity effect of Pu239 is the spectrum. This is at the position 1 softer than at the position 2 (Fig. 8). The reactivity effect is larger at the position 1 because the fission cross section of Pu239 increases at lower energies.

The difference in the reactivity effect of Fe_2O_3 (a scatterer) is mainly caused by the heterogeneity effect (Fig. 7). We noted before that neutrons with the energies of U238 resonances have been filtered out of the spectrum at position 2. A number of neutrons are scattered down to these energies by the sample. They have there a higher probability for absorption than before they collided with the sample. This is the effect described by C in the equation (2.2o).

The pronounced differences for Pu240 at the two positions are caused by the differences in the spectrum.[+)]

[+)] It is probably the first time that the reactivity effect of a pure Pu240 sample has been measured in a fast zero power reactor.

4.2 Comparison of the Theories

A series of calculations has been made with the SNEAK data set /38/ to test the different theories. These were the standard perturbation theory (P) /13/, the theory of E.A. Fischer (F) /15/,and the perturbation theory of integral transport theory with the ZERA code for the calculation of space-dependent resonance self-shielded reaction probabilities (O). The reactor is homogenized in the first and second theory; the plate structure is taken into account in the third treatment. The experimental results for different thicknesses and several isotopes at the two positions and the ratio of the calculated and experimental worths are given in the Table 1.

Isotope	Weight ,g	Position	Experiment in μ$/g	P/Exp.	F/Exp.	O/Exp.
U238	60	1	-37.7±0.4	0.97	0.93	1.16
	60	2	-24.4±0.2	1.49	1.44	1.26
	5	1	-86. ±3.	0.43	0.49	0.80
	5	2	-25. ±3.	1.42	1.63	1.22
Pu239	5	1	443. ±5.	0.98	1.01	1.09
	5	2	390. ±5.	1.13	1.15	1.19
Pu240	3	1	-170. ±5.	1.30	1.16	1.44
	3	2	-104. ±5.	2.13	1.93	1.77
Fe_2O_3	3	1	-22. ±5.		0.68	0.55
	3	2	-50. ±5.		0.30	0.52
U235	3	1	435. ±4.	1.00	1.00	1.00

Table 1: Comparison of Different Theories

Differences between the results of P and F exist for the small U238 samples and for the Pu240 samples. F accounts for elastic moderation and subsequent capture in sample or core. This gives a larger reactivity effect for U238 compared to P. For the larger samples this is off-set by the reduced effective cross section caused by self-shielding of the sample. The latter effect accounts also for the differences with Pu240.

The differences between O and the other two are due to two effects. First the self-shielding that is accounted for correctly and second,the spectra are calculated in a correct way at the different positions. The first effect explains the differences for Fe_2O_3, the latter for Pu240 and Pu239, and both effects together for U238.

4.3 Discrepancies Between Theory and Experiments

The discrepancies between theory and experiment are much smaller for the improved theory than for the other two. They are,however, still large compared to the standard deviations. This can be caused, as we noted in the introduction, by cross section errors in the data set used.

We have therefore repeated the calculations with some newer cross section sets /6/. The set PUO2RE is based on newer data for Pu239 and Pu240, e.g. the capture cross section of Pu240 has been lowered by a factor of two. The MOXTOT set is the PUO2RE set with a reduction in the capture cross sections of U238. The results are given in Table 2.

			Theory/Experiment		
Isotope	Weight, g	Position	SNEAK-Set	PUO2RE	MOXTOT
U238	60	1	1.16	1.13	0.95
	60	2	1.26	-	1.10
	5	1	0.80	0.80	0.72
	5	2	1.22	-	1.10
Pu239	5	1	1.09	1.04	1.04
	5	2	1.19	1.12	1.10
Pu240	3	1	1.44	0.98	0.91
	3	2	1.77	1.09	1.00
Fe_2O_3	3	1	0.55	0.55	0.55
	3	2	0.52	0.52	0.52

Table 2: Comparison of Different Data Sets

The results of the MOXTOT set are in best agreement with the experimental data. The agreement between theory and experiment is with a few exceptions better than 10%. In view of the variations in the calculated reactivity effects brought about by these cross section variations it should be possible to obtain agreement within the error limits of the experiment by adequate data adjustments.

The exceptions are the smallest U238 sample and the Fe_2O_3 sample. There are several explanations for the discrepancies of the U238 sample:

- The cross section of U238 should be lowered only down to 1 keV. The calculated reactivity would then increase for this sample and to a certain extend also that of the other U238 samples in the graphite but not so much that of the U238 at position 2.
- The accuracy of the reaction probabilities as calculated with the ZERA code: For small samples anomalous results have been found indicating that there is a limit on the accuracy (see appendix 2). This limit can be checked when the theory developed in chapter two has been programmed for the computer.
- The spectrum in the graphite is softer than calculated. This conclusion is also reached by Böhnel and Meister /36/ on the basis of other measurements.

The last assumption might improve the measurements at the position 2 too, since the normalisation is affected by the spectrum in the graphite. It may be brought about by the following:

The groupwidth of the cross section sets in use is large compared to the average lethargy gain per collison. The elastic moderation from one group to another is therefore determined only by the number of neutrons in the lower end of the groups. This is accounted for by condensing the groups with a given weighting spectrum. The spectrum of 5C is softer than the weighting spectrum used for the cross section sets. The elastic moderation cross sections will therefore be too small. An increase in the moderation cross sections results in a softer spectrum.

The discrepancies of Fe_2O_3 may also be explained by elastic moderation cross sections that are too small

5. CONCLUSIONS

Sample size and heterogeneity effects in heterogeneous fast reactors with soft spectra are not accounted for correctly with the methods presently in use. It has been shown that the theory developed in this study can describe these effects qualitatively and to a large extend also quantitatively.

A correct description of the experiments is only possible if the slab geometry of the reactor lattice is only slightly perturbed by the experimental equipment. This is achieved by the newly devised pile-oscillator element. The fact that fuel moves in the reactor necessitated an extension of the inverse kientics method.

It has been demonstrated that high precision reactivity measurements are possible with this equipment and method.

The discrepancies between this theory and the experiments can be explained by cross section errors. Reactivity worth experiments are thus a powerful method for the testing of cross section data.

ACKNOWLEDGEMENT

The author acknowledges the support of EURATOM and the Gesellschaft für Kernforschung that enabled him to perform this study.

A P P E N D I X 1

The time-dependent reactor equations can be written as

1) $S = (1-\beta)\cdot(F+\delta F)S_t + (M+\delta M)S_t + D + S_s$

where
- S the new source after a collision
- S_t the old source
- $F+\delta F$ the fission matrix $F_{ij}^{mn} = \chi_j \cdot P_{fi}^{nm}$
- $M+\delta M$ the scattering matrix $M_{ij}^{mn} = P_{i\to j}^{nm}$
- D the delayed neutrons source $D = \sum_i \lambda_i C_i$
- S_s the spontaneous source.

The matrices contain delay times that are the flught times of the neutrons between the collision. They are not given explicitly here.

For a stationary reactor

2) $S-FS-MS = 0$

3) $S^+-F^+S^+-M^+S^+ = 0$

The adjoint condition requires that

4) $< YX-YFX-YMX-YX+XF^+Y+XM^+Y > = 0$

where $< >$ denotes the integral over the whole reactor and all energies

Eq. 4 holds for all functions X and Y.

If we multiply Eq. 3 with S_t and apply the adjoint condition we obtain

5) $< S^+S_t-S^+FS_t-S^+MS_t > = 0.$

Multiplying Eq. 1 with S^+ integrating over space and energy and subtracting Eq. 5 we obtain

6) $< S^+(S-S_t) > = < S^+\delta FS_t > + < S^+\delta MS_t > - < S^+\beta(F+\delta F)S_t > + D+S_s$

We define a multiplication factor so that $k = 1/\lambda$

7) $S_t = \lambda(F+\delta F)S_t+(M+\delta M)S_t.$

We apply to this equation the normal operations to obtain a peturbation equation and get

8) $$0 = \langle S^+(\lambda-1)(F+\delta F)S_t \rangle + \langle S^+\delta F S_t \rangle + \langle S^+\delta D S_t \rangle .$$

This is an exact formulation of perturbation theory since the perturbed sources are used.

If we substitute Eq. 8 in Eq. 6 we obtain

9) $$\langle S^+(S-S_t) \rangle = (1-\lambda) \langle S^+(F+\delta F)S_t \rangle - \langle S^+,\beta(F+\delta F)S_t \rangle + D+S_s .$$

To transform this formula into point kinetics we have to noramlize the source distributions

10) $$S = S_o(t)\cdot A(t) \quad \text{with the condition} \quad \frac{\partial}{\partial t} \langle S^+ S_o \rangle = 0.$$

We can now write Eq. 11

11) $$(A(t) - A(t-\Delta t)) \cdot \langle S^+ S_o \rangle = (1-\lambda)A(t-\Delta t) \cdot \langle S^+(F+\delta F)S_o \rangle - A(t-\Delta t) \cdot \langle S^+\beta(F+\delta F)S_o \rangle + D+S_s$$

Where Δt, the mean time between collisions for the neutrons, is $\Delta t = 1/\lambda_t$. Since this time in the reactor is short we can write

12) $$\frac{d}{dt}\frac{1}{\lambda_t}\langle S^+ S_o \rangle = (1-\lambda)A \cdot \langle S^+F+\delta F S \rangle - A \langle S^+\beta(F+\delta F)S_o \rangle + D+S_s .$$

We define now the lifetime, the effective precursor concentration, and the effective spontaneous source

13) $$\Lambda = \frac{1}{\lambda_t} \cdot \frac{\langle S^+ S_o \rangle}{\langle S^+(F+\delta F)S_o \rangle}$$

14) $$C_i^{eff} = \frac{1}{\lambda_t} \cdot \frac{\langle S^+ C_i \rangle}{\langle S^+ S_o \rangle} = \frac{\langle S^+ C_i \rangle}{\langle S^+(F+\delta F)S_o \rangle} \cdot \frac{1}{\Lambda}$$

15) $$S_s^{eff} = \frac{1}{\lambda_t} \frac{\langle S^+ S_s \rangle}{\langle S^+ S_o \rangle} = \frac{\langle S^+ S_s \rangle}{\langle S^+(F+\delta F)S_o \rangle} \frac{1}{\Lambda}$$

Substitution of these definitions into Eq. 12 gives us

16) $$\frac{dA}{dt} = \left(\frac{k-1}{k} - \beta\right) \cdot \frac{A(t)}{\Lambda} + C_i^{eff} + S_s^{eff} .$$

If the reactor behaves like a point reactor C_i^{eff} may be calculated

17) $$\frac{dC_i^{eff}}{dt} = \frac{\beta_i}{\Lambda} \cdot A(t) - \lambda_i C_i^{eff} .$$

In the case of stationary fuel is the change in the precursor concentration given by

18) $$\frac{dC_i}{dt} = \beta_i \, (F+\delta F) \, S - \lambda_i C_i ,$$

in the case of moving fuel

19) $$\frac{dC_i}{dt} = \beta_i \, (F+\delta F) \, S - \lambda_i C_i - (\nabla C_i, \vec{V}).$$

The last term of Eq. 19 denotes the net loss of precursors by the moving fuel.

In the computer program KINEMAT Eq. 19 is solved digitally with the assumption that the fission rate distribution remains constant. With Eq. 14 the effective precursor concentration is calculated. Then equation 16 is solved by the inverse kinetics method.

From a reactor calculation the value

2o) $$\frac{S^+(F+\delta F)S}{< S^+(F+\delta F)S >} = F_r$$

is determined; this is the statistical weight.

The precursor concentration may then be written as

21) $$\frac{dC_i^n}{dt} = \beta_i \cdot \frac{F_r \cdot A(t)}{S^+ \Lambda} - \lambda_i C_i - (\nabla C_i^n, \vec{V})$$

where C_i^n is the normalized precursor concentration. Eq. 14 then becomes

22) $$C_i^{eff} = < S^+ C_i^n > .$$

If the reactor is stable then Eq. 16 becomes

23) $$\frac{dA}{dt} = 0 \qquad \left(\frac{k-1}{k} - \beta\right) \cdot \frac{A}{\Lambda} = -S_s^{eff} .$$

Since k-1/k can be measured in $, e.g. with a calibrated control rod, $k-1/k = \rho \cdot \beta$ Eq. 23 becomes

$$24)\quad \frac{S_s \cdot S^+}{< S^+(F+\delta F)S >} = -\rho \cdot \beta \cdot A_s \ .$$

We need the value $\frac{S^+(F+\delta F)S}{< S^+(F+\delta F)S >}$ to compare theory and experiment.

Since the detector signal is not normalized a normalisation is made by means of a fission rate measurement. This measurement showed that $1/\nu$ fissions per second in the central cm^3 are equal to A_f counts per second of the detector.

From the effective source determination - the spontaneous source and the reactivity of the source can be eliminated by separate measurements - the worth of 1 fission neutron can be determinded

$$25)\quad \frac{S^+}{< S^+(F+\delta F)S >} = -\frac{A_s}{S_s} \cdot \rho \cdot \beta$$

with the normalisation of the detector signal

$$26)\quad \frac{S^+(F+F)S}{< S^+(F+F)S >} \cdot \frac{1}{\beta} = \frac{A_s}{A_f} \cdot \frac{1}{S_s} \cdot \rho \cdot \frac{1}{\nu} \ .$$

Thus the ratio of the normalisation integral and the effective delayed neutron fraction can be determined by an effective source determination and an absolute fission rate measurement with the same detector.

APPENDIX 2

The Calculation of the Reaction Probabilities with the ZERA Code

The reaction probability for a reaction of type x in the isotope y at r from neutrons with the energy of group i starting at r' is given by

$$1) \quad P_{xi}\ (r' \to r) = N^y(r) < \sigma_x^y(u)\ \frac{e^{-1}}{4\pi\ |r-r'|^2} >_i$$

where the symbols have the meaning as defined in chapter 2. The ZERA code calculates the reaction probabilities

$$2) \quad P_{xi}^y\ (r' \to r) = \int_o^\infty \alpha_x^y\ (\sigma_o,\ r' \to r)\ \frac{\sigma_x^y\ (\sigma_o)}{\sigma_t^y\ (\sigma_o)+\sigma_o}\ d\sigma_o$$

where the α_x^y are the inverse Stieltjes transform of the transmission between r and r'.

$$3) \quad \frac{e^{-1^y}}{4\pi|r-r'|^2} = \int_o^\infty d\sigma_o\ \frac{\alpha_x^y(\sigma_o, r' \to r)}{\sigma_t^y+\sigma_o}$$

$$4) \quad 1^y = \int_r^{r'} dr''\ \Sigma_t^y(r'')$$

Wintzer uses

$$5) \quad \Sigma_t^y(r'') = N^y(r'')\ \{\sigma_t^y+\sigma_o^y(r'')\}$$

The σ_o^y are calculated with the self-shielding factors for the homogeneous medium.

The neutron balance requires that the collision probability for all isotopes equals the attenuation

$$6) \quad \sum_{z=1}^{Y} P_{ti}^y(r' \to r) = N^y(r)\ (\sigma_{oi}^y + <\sigma_t^y>_i)$$

or

$$7) \quad \sum_{\substack{z=1 \\ z \neq y}}^{Y} P_{ti}^z(r' \to r) = N^y(r)\ \sigma_{oi}^y$$

The Eq. 7) is not necessarily true since the σ^{y}_{oi} are calculated in advance, and the collision probabilities P^{z}_{ti} are calculated according to the equations 3) and 2).

It showed that a normalisation is necessary in order to keep the neutron balance in equilibrium.

The reaction probabilities must be normalized according to

$$8) \quad P^{y}_{xi}(r'\to r)_{\text{normalized}} = \frac{P^{y}_{xi}(r'\to r)}{\int_{o}^{\infty} dV \sum_{z=1}^{Y} P^{z}_{ti}\,(r'\to r)} \quad .$$

The normalisation causes a correction up to a few percent in the reaction probabilities. Theses corrections may cause large inaccuracies as we use differences in reaction probabilities.

In the theory of chapter 2 the condition of the neutron balance is fulfilled. This can be shown be reorganizing the Eq. 2.6

$$9) \quad P_{ti}(r'\to r) = \sum_{y=1}^{Y} \sum_{k=2}^{K} \alpha_i^{yk} \{\sigma^{yk}_{ti} + \sum_{\substack{z=1 \\ z\neq y}}^{Y} N^{z}\,\sigma^{zl}_{ti}\} \cdot \frac{e^{-1_i^{yk}}}{4\pi\,|r'-r|^2} +$$

$$+ (1- \sum_{y=1}^{Y} \sum_{k=2}^{K} \alpha_i^{yk}) \cdot (\sum_{z=1}^{Y} N^{z}\,\sigma^{zl}_{ti}) \frac{e^{-1_i^{zl}}}{4\pi|r'-r|^2}$$

$$10) \quad \Sigma^{yk}_{ti} = N^{y}\,(\sigma^{yk}_{ti}+\sigma^{y}_{o}) = N^{y}\,\sigma^{yk}_{ti} + \sum_{\substack{z=1 \\ z\neq y}}^{Y} N^{z}\,\sigma^{zl}_{ti}$$

so that the correct attenuation is used for the different contributions to the reaction probability.

References

/1/ P. ENGELMANN et al., Fast Reactor Physics Vol. II, p. 36, IAEA, Vienna 1968

/2/ H. ANDERSON, E. FERMI, A. WATTENBERG, G. WEIL, W. ZINN, Phys. Rev. 72, p. 16-23 (1947)

/3/ A.v.d. HONERT, Atoomenergie en haar toepassingen 11, p. 45 (1969)

/4/ K.P. BACHUS, C.B. v.d. DECKEN, W. RAUSCH, Trans. Am. Nucl. Soc. 11, p. 567 (1968)

/5/ W.C. REDMAN and M.M. BRETSCHER, Nucl. Sci. and Eng. 27, p. 34-44 (1967)

/6/ E. KIEFHABER et al."Evaluation of Fast Critical Experiments by Use of Recent Methods and Data" Proceedings of the BNES Conf. on"The Physics of Fast Reactor Operation and Design", London, June 24-26, 1969

/7/ J.J. SCHMIDT, "Neutron Cross Sections for Fast Reactor Materials" KFK-120, Part I and II (1966)

/8/ E.D. PENDLEBURY et al. "The Optimization of Neutron Cross Section Data Adjustments to Give Agreement with Experimental Critical Sizes" ANL-7320, p. 88 (1966)

/9/ J.L. ROWLANDS et al., "Adjustment of Nuclear Data to Fit Integral Experiments" Proceedings of the BNES Conf. on"The Physics of Fast Reactor Operation and Design", London, June 24-26, 1969

/10/ J.Y. BARRE and J. RAVIER, Fast Reactor Physics Vol. I, p. 205, IAEA, Vienna 1968

/11/ J.Y. BARRE et al. "Lessons Learnt from Integral Experiments on a Set of Multigroup Cross Sections" Proceedings of the BNES Conf. on "The Physics of Fast Reactor Operation and Design", London, June 24-26, 1969

/12/ M. BUSTRAAN, Fast Reactor Physics, Vol. I, p. 349, IAEA, Vienna 1968

/13/ R. BÖHME et al., Fast Reactor Physics, Vol. II, p. 67, IAEA, Vienna 1968

/14/ I.I. BONDARENKO et al. "Group Constants for Nuclear Reactor Calculations" Consultants Bureau, New York (1964)

/15/ E.A. FISCHER, "A Method to Calculate Reactivity Worth by Integral Transport Theory", KFK-995 (1969)

/16/ ANL-7527, Reactor Development Programm Progress Report Dec. 1968, p. 23-29

/17/ P.E. McGRATH and W.K. FOELL, Trans. Am. Nucl. Soc. 12, p.188 (1969)

/18/ P. KIER, "A Method of Computing Resonance Integrals in Multirigion Reactor Cells", Int. Conf. on Research Reactor Utilization and Reactor Mathematics, Mexico City 1967

/19/ ANL-7548, Reactor Development Programm Progress Report, January 1969, p. 8

/20/ Panel of the BNES Conf. on "The Physics of Fast Reactor Operation and Design", London, June 24-26, 1969

/21/ E.A. FISCHER, "Interpretation of Doppler Coefficient Measurements in Fast Critical Assemblies", ANL-7320, p. 350-357 (1966)

/22/ D. WINTZER, Fast Reactor Physics, Vol. II, p. 237, IAEA, Vienna 1968

/23/ S.G. CARPENTER, Nucl. Sci. and Eng. 21, p.429 (1965)

/24/ A.M. WEINBERG and E.P. WIGNER, "The Physical Theory of Neutron Chain Reactions", The University of Chicago Press, p. 187, 1958

/25/ L. DRESNER, "Resonance Absorption in Nuclear Reactors" Pergamon Press Oxford, p. 19 (1960)

/26/ J. CODD and P. COLLINS, "Some Calculations Concerning the Influence of Resonance Overlapping on the Doppler Effect in a Dilute Fast Reactor" ANL-6792, p. 711,(1963)

/27/ J.E. BEARDWOOD, A.J. CLAYTON, "The Solution of the Transport Equation by Collision Probability Methods", ANL-7050 (1965)

/28/ J. CARLVIK, "A Method for Calculating Collision Probabilities in General Cylindrical Geometry and Applications to Flux Distributions and Dancoff Factors" A/Conf. 28/P/681

/29/ R. BONALUMI, Energie Nucleare 8, p. 326 (1961)

/30/ D. WINTZER, "Zur Bestimmung von Heterogenitätseffekten in periodischen Zellstrukturen thermischer und schneller Reaktoren", KFK-743 (1969)

/31/ A. ERDELYI et al., "Tables of Integral Transforms" McGraw Hill, New York, 1954

/32/ G. BITELLI et al., "Analysis and Correlation of Integral Fast Experiments in Fast Reactors with Nuclear Parameters" Proceedings of the BNES Conf. on "The Physics of Fast Reactor Operation and Design", London, June 24-26, 1969

/33/ E.A. FISCHER, "Interpretation von Dopplerproben-Messungen in schnellen kritischen Null-Energie-Anlagen, KFK-844 (1969)

/34/ D. STEGEMANN et al., Fast Reactor Physics Vol. II, p. 79, IAEA, Vienna 1968

/35/ H. BORGWALDT et al., "Experience Obtained at Karlsruhe with Different Kinetic Methods of Reactivity Determination", KFK-899 (1968)

/36/ K. BÖHNEL and H. MEISTER, "A Fast Reactor Lattice Experiment for Investigation of k_∞ and Reaction Rate Ratios in SNEAK, Assembly 5" KFK-Report in preparation

/37/ C.E. COHN, Nucl. Sci. and Eng. 7, p. 472-475 (1960)

/38/ H. HUSCHKE, "Gruppenkonstanten für Dampf- und Natrium-gekühlte schnelle Reaktoren in einer 26 Gruppendarstellung", KFK-770 (1968)

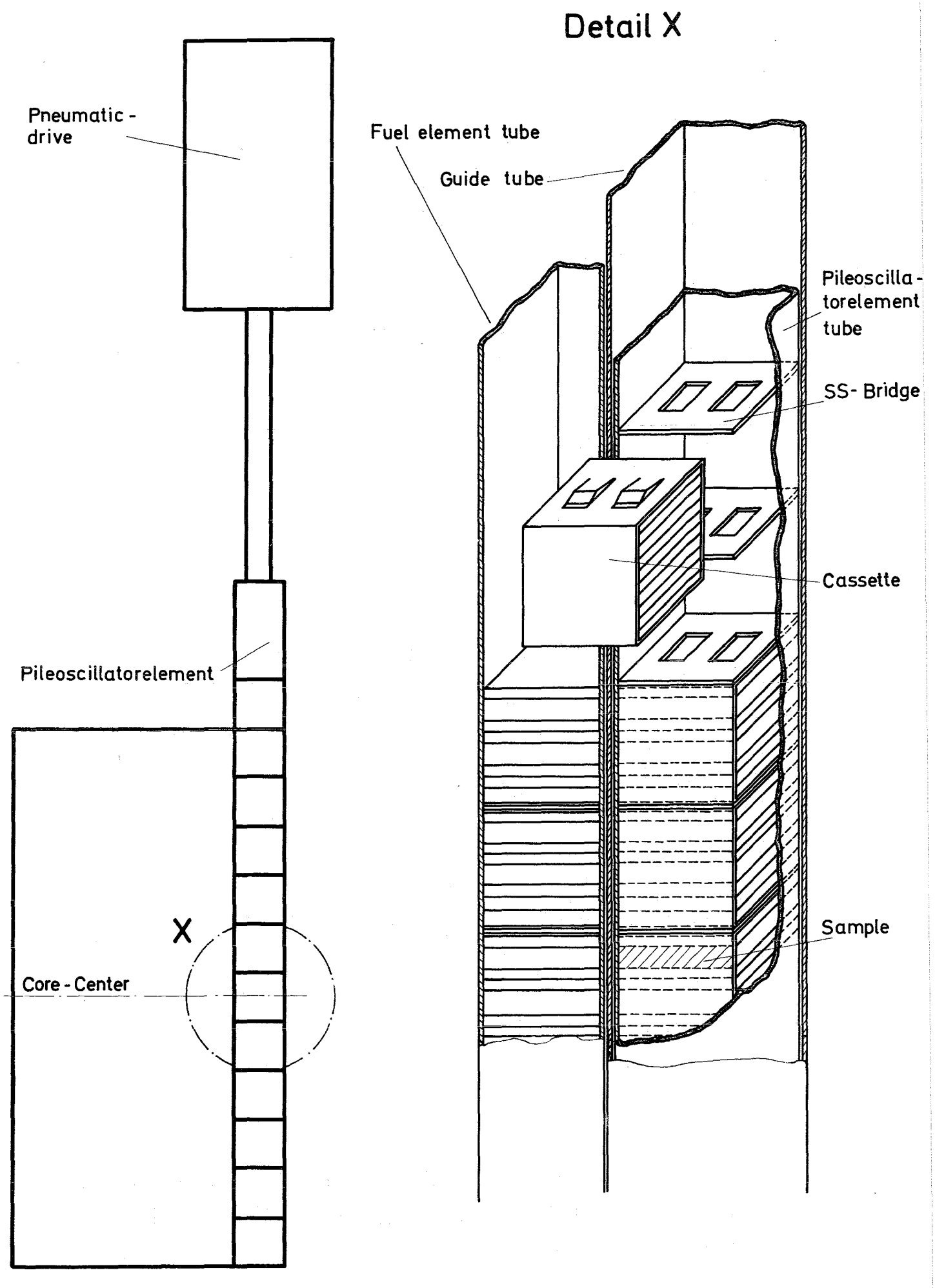

Fig. 1 Exploded view of pileoscillator element

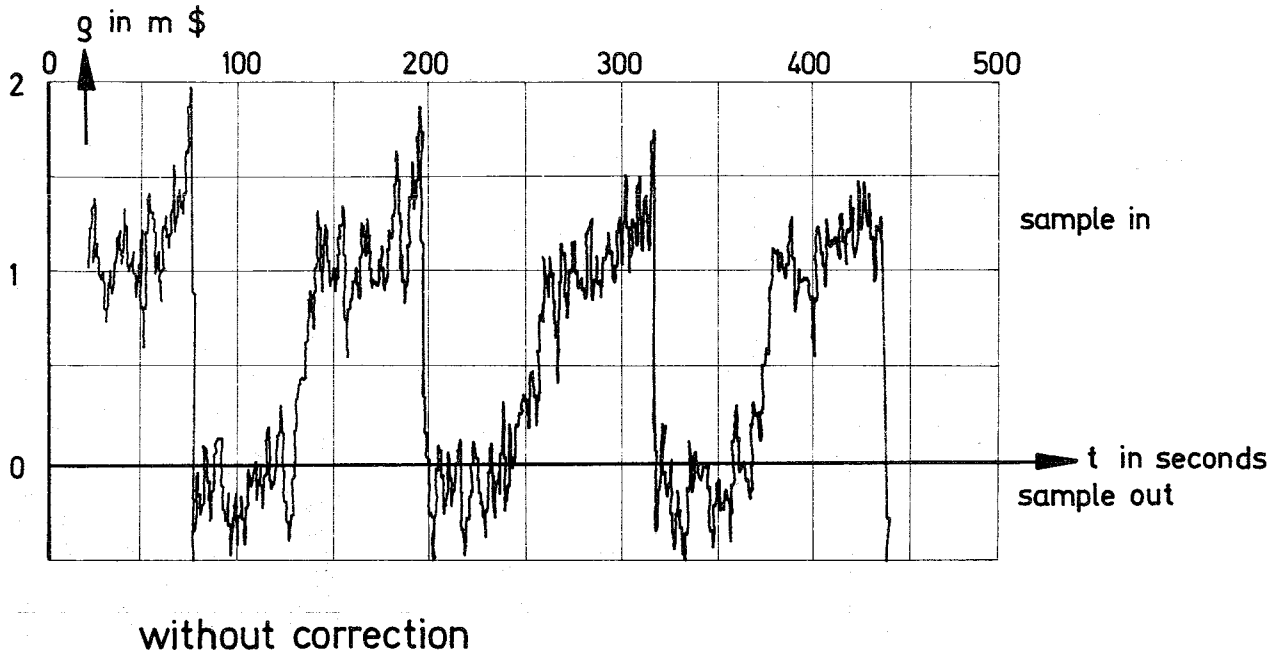

without correction

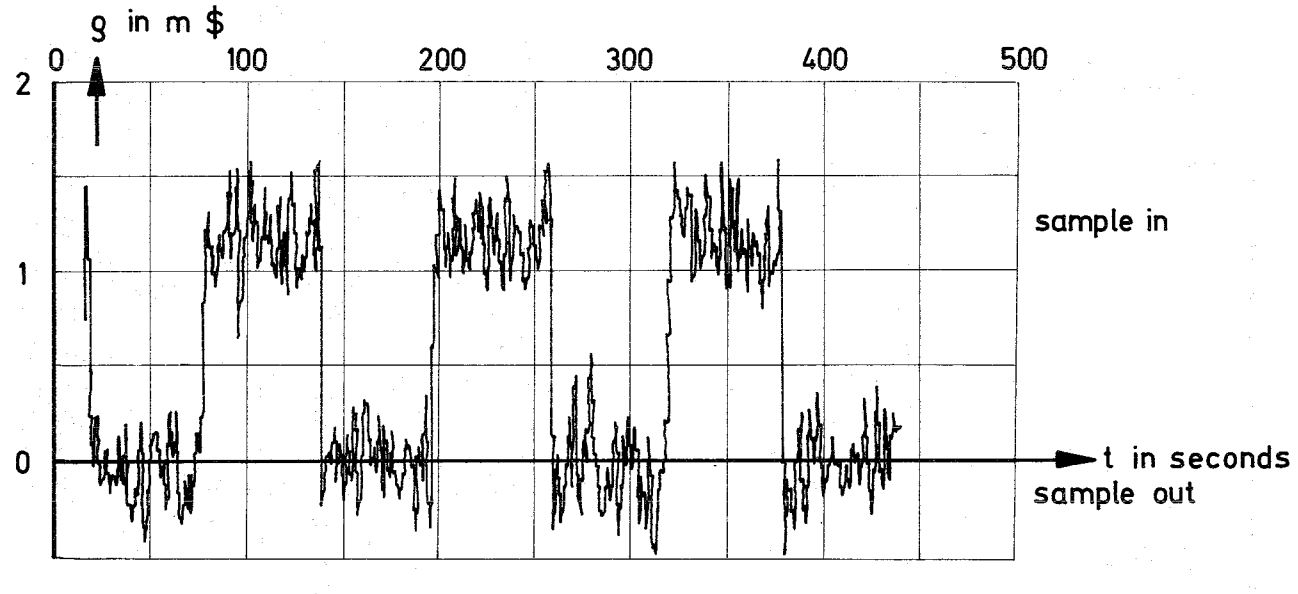

with correction

Fig.2 The reactivity as function of time with and without a correction for the transport of precursor nuclei.

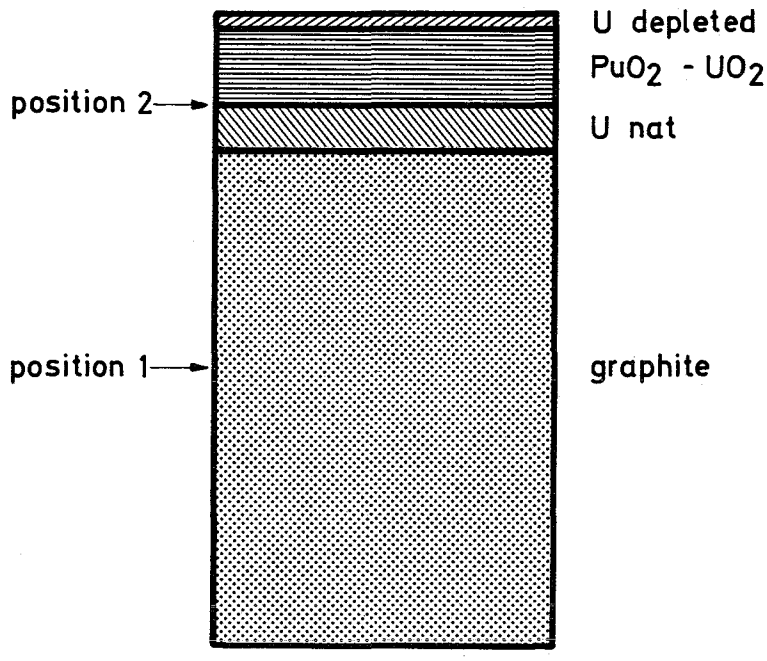

Principal cell structure of SNEAK 5C

Fig. 3

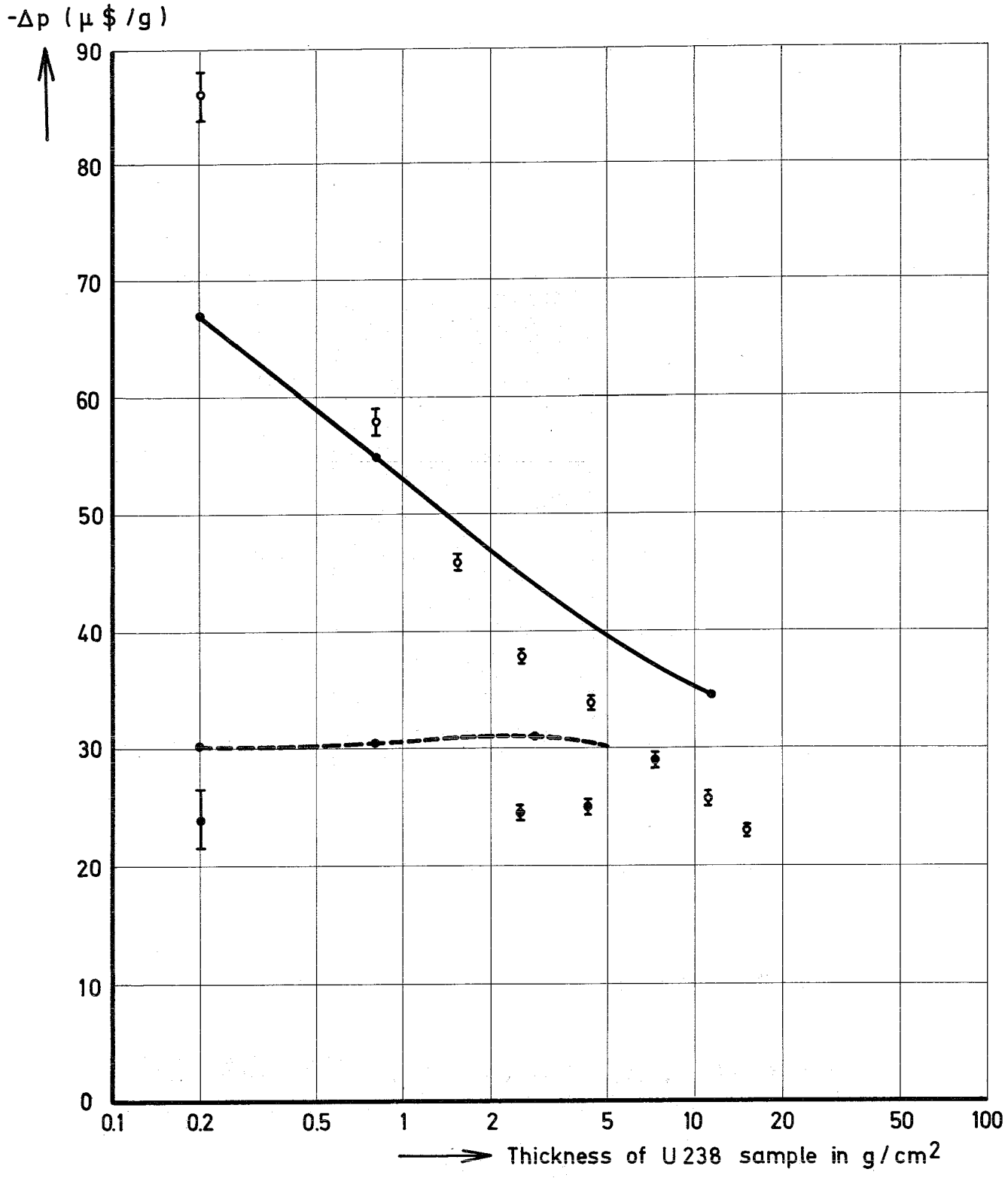

Fig. 4 Central Reactivity Worth of U 238 in SNEAK 5C

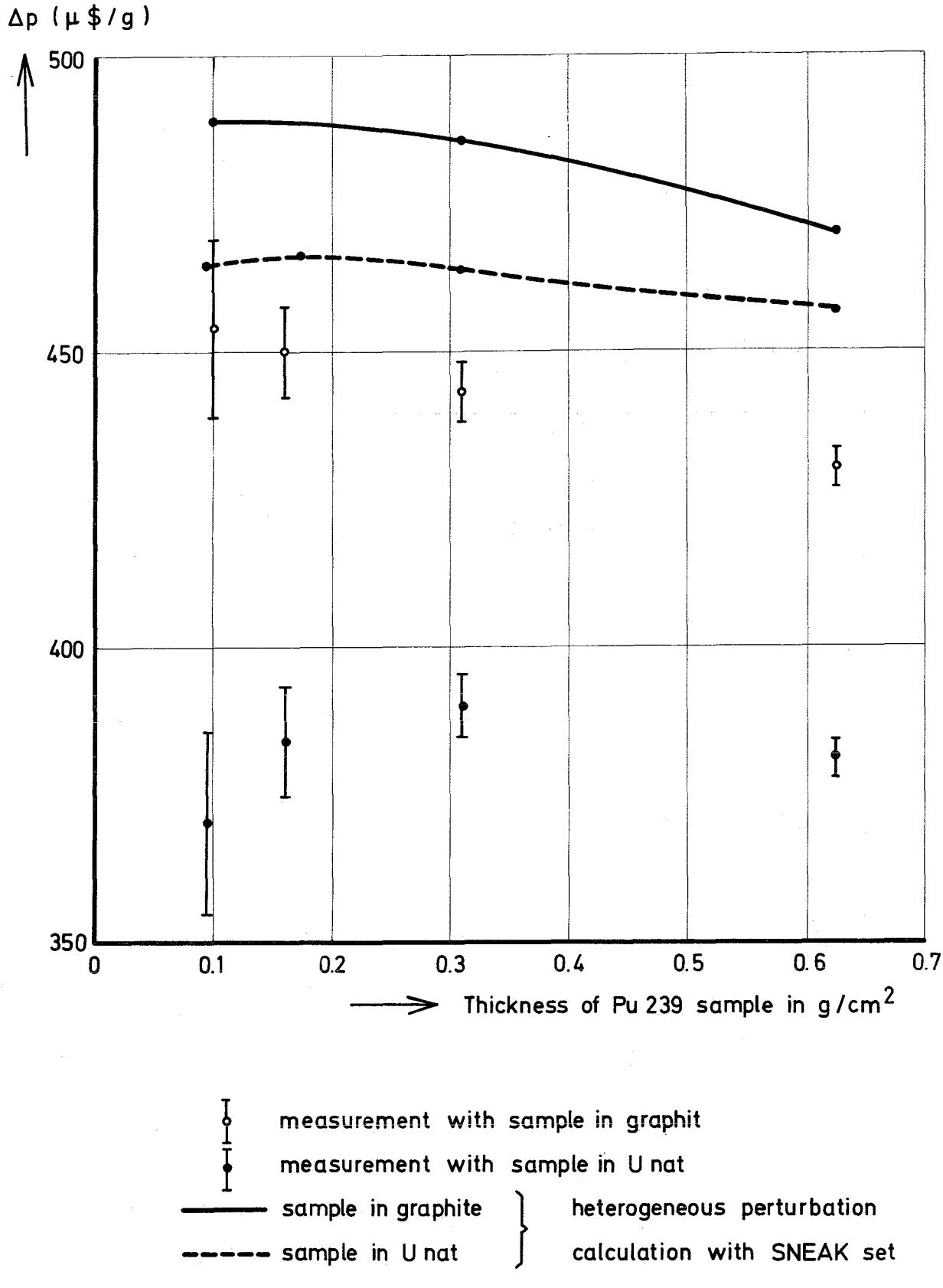

Fig. 5 Central Reactivity Worth of Pu 239 in SNEAK 5C

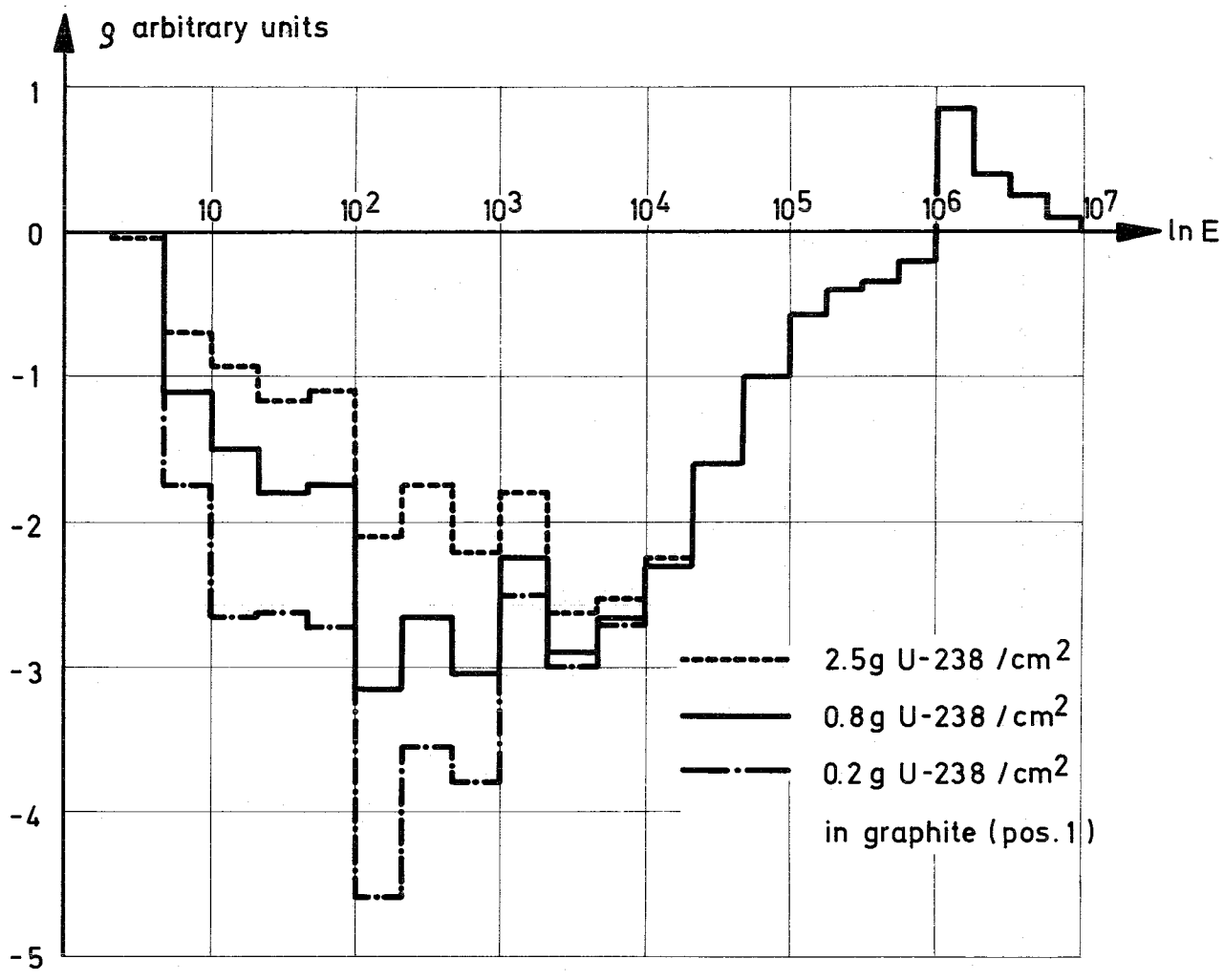

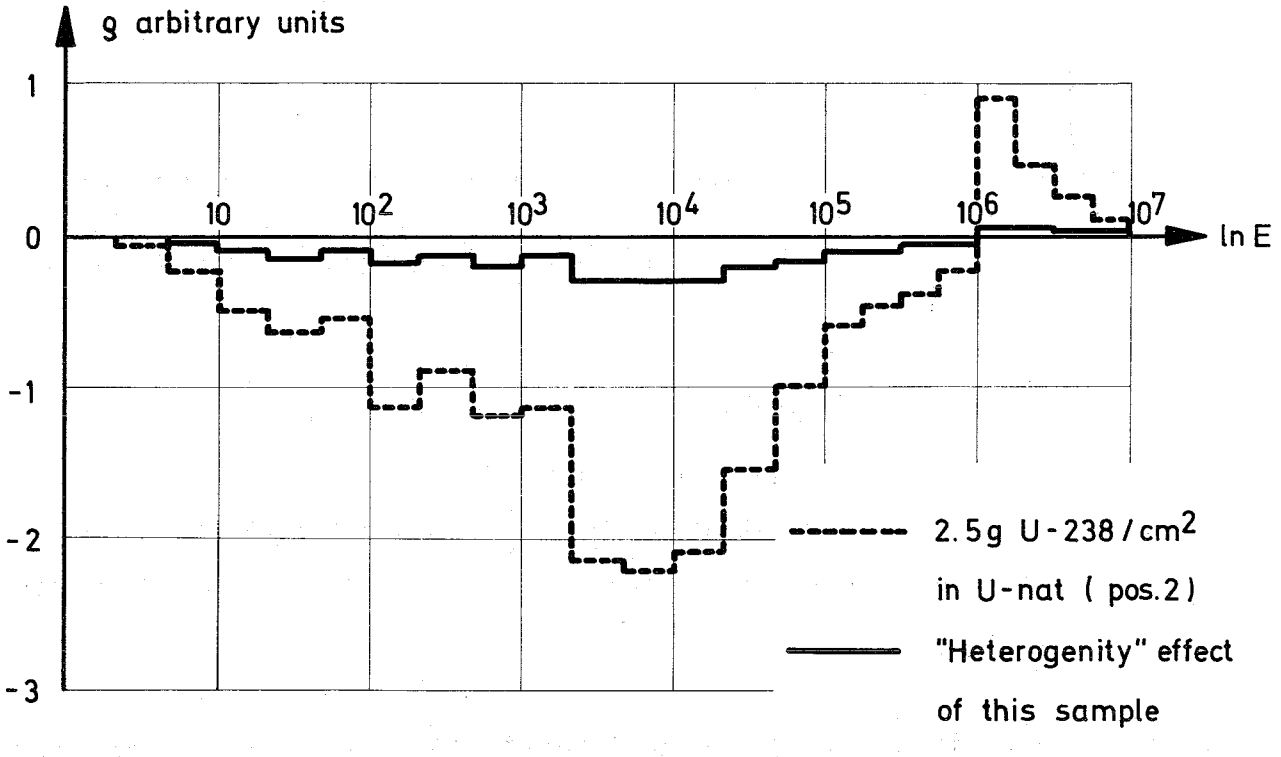

Fig. 6 The reactivity effect of U-238 as a function of energy

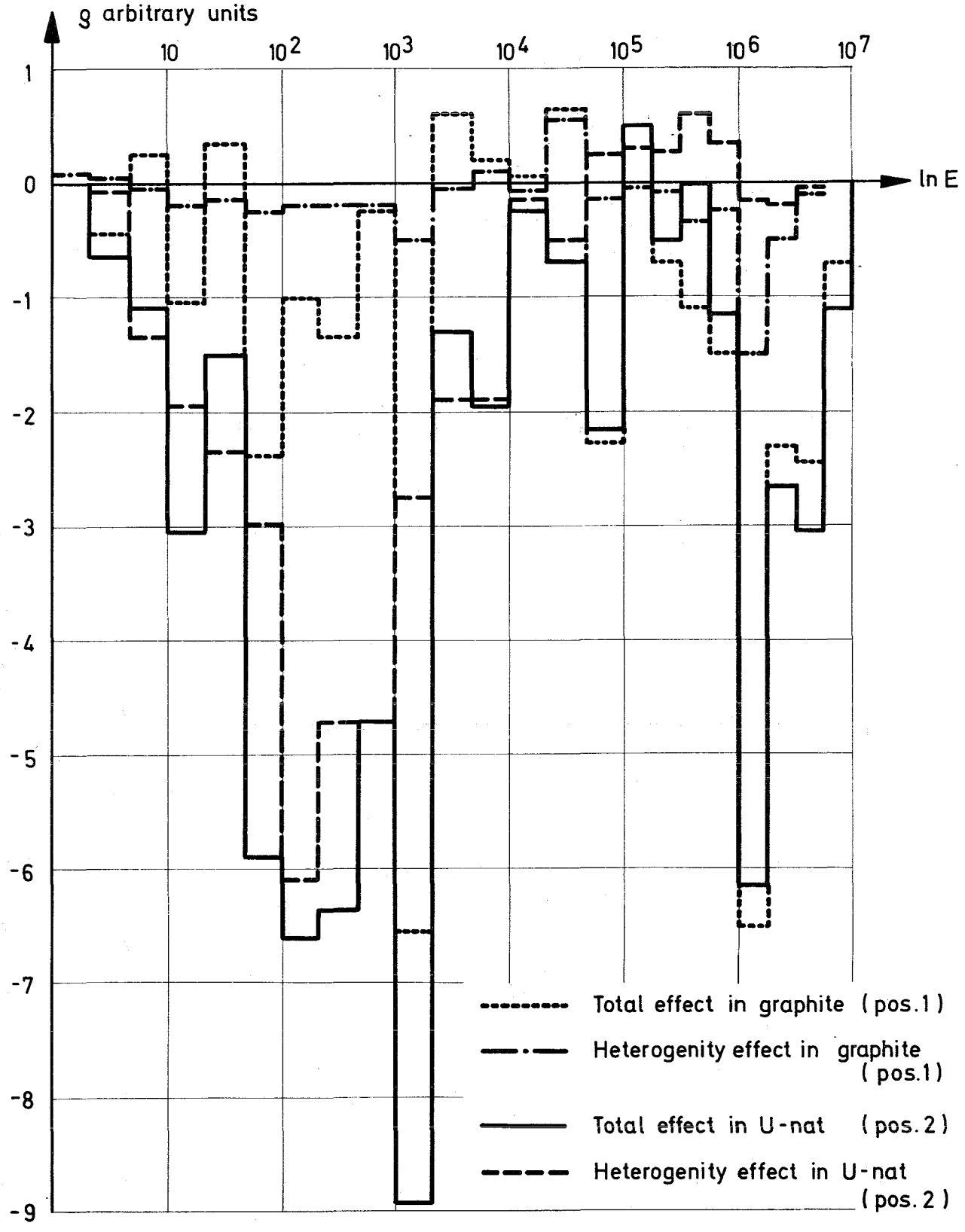

Fig.7 The reactivity effect of Fe_2O_3 as a function of energy

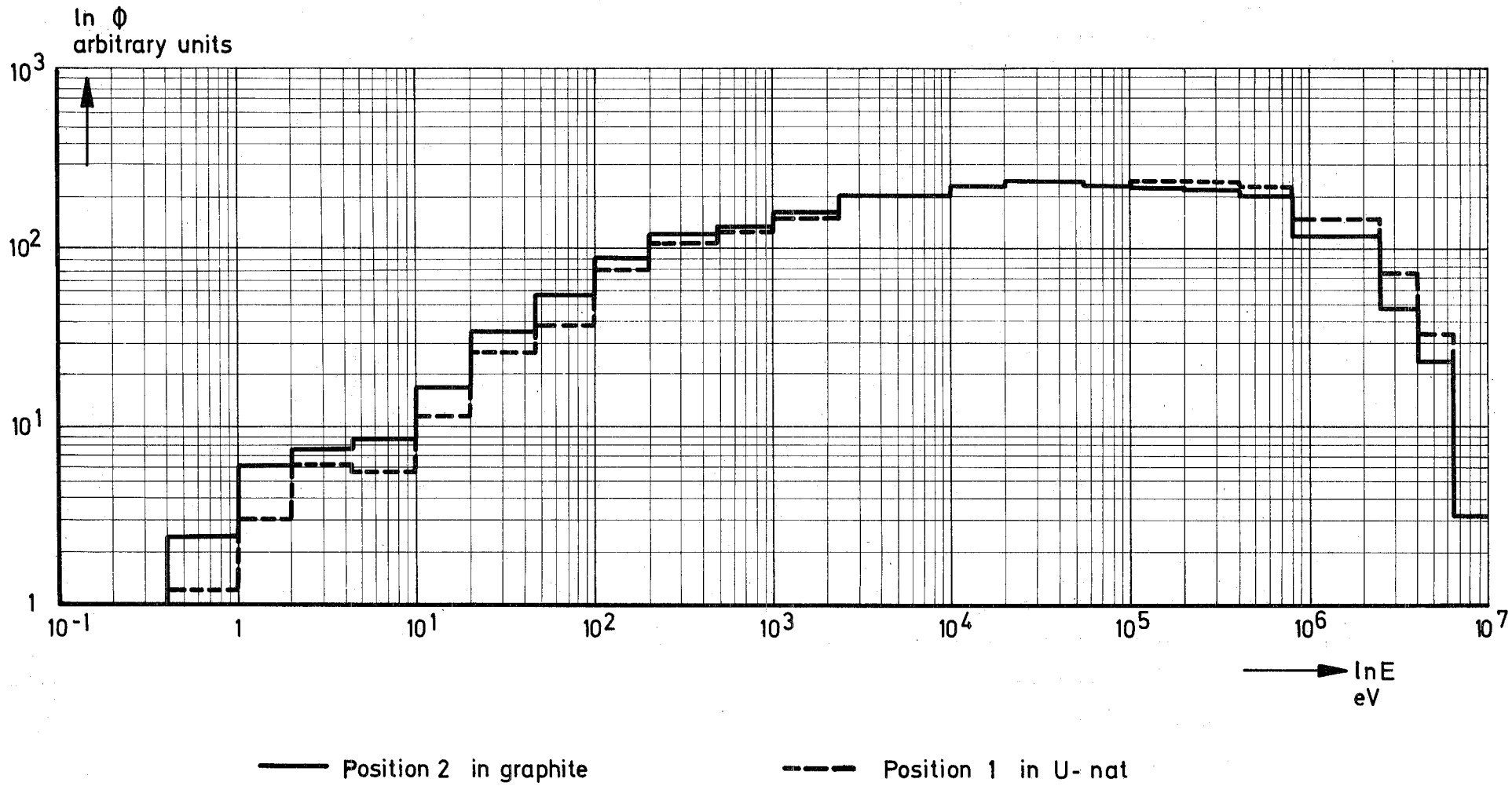

Fig. 8 The neutron spectrum in SNEAK 5C